



Contents lists available at ScienceDirect

## Chemical Physics Letters

journal homepage: [www.elsevier.com/locate/cplett](http://www.elsevier.com/locate/cplett)

## Electronic structure and luminescence center of blue luminescent carbon nanocrystals

Jigang Zhou<sup>a,c,\*</sup>, Xingtai Zhou<sup>a</sup>, Ruying Li<sup>b</sup>, Xueliang Sun<sup>b</sup>, Zhifeng Ding<sup>a</sup>, Jeffrey Cutler<sup>c</sup>, Tsun-Kong Sham<sup>a</sup>

<sup>a</sup> Department of Chemistry, The University of Western Ontario, London, ON, Canada N6A 5B7

<sup>b</sup> Department of Mechanical and Materials Engineering, The University of Western Ontario, London, ON, Canada N6A 5B7

<sup>c</sup> Canadian Light Source, University of Saskatchewan, Saskatoon, Canada S7N 0X4

## ARTICLE INFO

## Article history:

Received 29 November 2008

In final form 28 April 2009

Available online 3 May 2009

## ABSTRACT

The electronic structure and the origin of luminescence from blue luminescent carbon nanocrystals (CNC) have been investigated with X-ray absorption near-edge structures (XANES) and X-ray excited optical luminescence (XEOL). XANES shows that nitrogen has been incorporated into the carbon nanocrystals matrix (dominated by  $sp^2$  carbon). XEOL from CNC is compared with that from natural diamond and previously reported CVD nanodiamond containing N impurities. The results reveal that N doping is almost certainly responsible for the blue luminescence in carbon nanocrystals. The implication of the results is discussed.

© 2009 Elsevier B.V. All rights reserved.

Carbon nanostructures such as fullerene, carbon nanotubes (CNTs) and nanodiamond film are attractive building blocks in the fabrication of important optoelectronic devices, for instance, sensors, field emitters and light emitting applications [1,2]. Luminescent carbon nanostructure also has the unique promise for high efficient photoluminescence in light-emitting devices and low toxicity in the biology labeling and biomedicine [3–9].

To render carbon nanostructures luminescence, the functionalization of fullerene, CNTs and graphite nanoparticles [4,5,7–10] appears to be a more desirable approach compared to laser ablation of bulk graphite [11]. Electrochemical treatment of CNTs has been demonstrated to be another effective avenue in making highly efficient blue luminescent carbon nanocrystals [3]. The elucidation of the electronic structure and the origin of luminescence from these emitters are crucial to their applications. It has been noted that the  $sp^2$  rich phase in a  $sp^3$  matrix contributed to the luminescence in the nanostructured carbon thin film [11]. Because of the strong electron affinity of fullerene and single walled CNTs (SWCNTs), the visible luminescence from their derivatives has been attributed, for example, to charge redistribution between the amine group in the amine-containing passivating molecule and the targeted carbon nanostructure [6,7]. Such interaction is believed to produce an emissive adduct. The solvatochromic effect of the luminescence of the derivative on the solvent provides experimental evidence supporting this explanation [6,7]. Surface energy state stabilization by passivation has been used as a model in understanding this luminescence [4,5]. However the electronic structure

of the luminescent carbon nanostructures has not been reported. Further, the above-mentioned model for the origin of the luminescence needs to be verified experimentally.

This report applies X-ray absorption near-edge structure (XANES) and X-ray excited optical luminescence (XEOL) to elucidate the electronic structure and the origin of the blue luminescence from carbon nanocrystals (CNCs), which were produced by the electrochemical method reported recently [3]. Briefly, the CNCs were prepared from multiwalled CNTs coated on a carbon paper electrode in a degassed acetonitrile solution with a 0.1 M tetrabutylammonium perchlorate (TBAP) as the supporting electrolyte, by cycling the potential from  $-2$  V to 2 V. The high resolution transmission electron microscopy (HRTEM) image in Fig. 1 shows the uniform morphology and size ( $\sim 3$  nm in diameter) distribution of the CNCs. The CNCs collected from the solution were further purified by aqueous extraction (removing the TBAP) before depositing onto a Si wafer. The specimen thus prepared was used in the XANES and XEOL measurements at room temperature. We have also made same measurements on a natural diamond sample (0.39 carat, from Sierra Leone), which appears opaque yellow indicative of N impurities.

XANES measures the modulation of the atomic X-ray absorption cross-section across a given edge (core level excitation threshold, e.g. C and N K-edge) of an element in a chemical environment and is element and oxidation state specific. XANES has been successfully applied to investigate many problems concerning chemical bonding, electronic structure, surface chemistry and CNTs orientation [2,12–16]. As an optical spectroscopy excited by X-ray photons, XEOL is an X-ray photon-in, optical photon-out technique and it investigates the conversion of X-ray energy absorbed by a material into optical emission. We can probe energy, charge

\* Corresponding author. Address: Canadian Light Source, University of Saskatchewan, Saskatoon, Canada S7N 0X4.

E-mail address: [jigang.zhou@lightsorce.ca](mailto:jigang.zhou@lightsorce.ca) (J. Zhou).

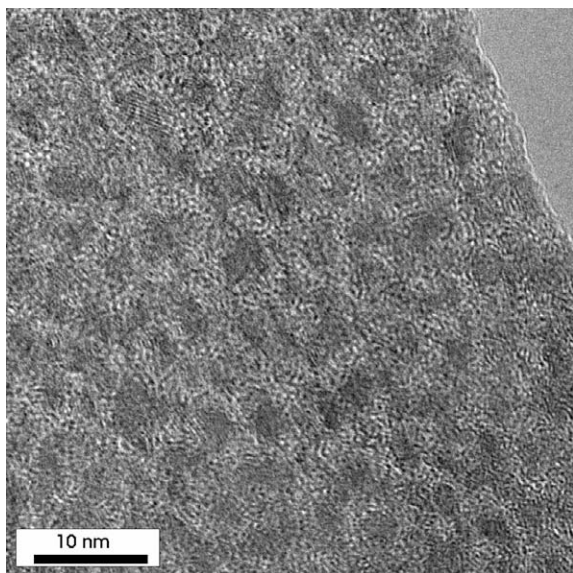


Fig. 1. HRTEM of purified carbon nanocrystals.

and spin transfer by monitoring the XEOL. By Scanning the excitation energy across an absorption edge, XEOL can be site and excitation channel sensitive, providing a unique advantage in elucidating the origin of luminescence in a complex nanostructure [2,3,17].

XANES and XEOL at the C and N K-edge were performed at the spherical grating monochromator (SGM) undulator beamline at the Canadian Light Source (CLS), a 2.9 GeV, third generation synchrotron facility located in Saskatoon. The energy resolution ( $\Delta E/E$ ) is  $\sim 2 \times 10^{-4}$  over the photon energy range from 250 to 1500 eV. XANES were recorded simultaneously in total electron yield (TEY) and fluorescence yield (FY), using specimen current and a multichannel plate detector, respectively. The XANES spectra were normalized to the incident photon flux,  $I_0$ , using an Au mesh, refreshed by Au evaporation prior to the measurement. XEOL was recorded using a JY 100 monochromator (200–850 nm) equipped with a Hamamatsu R-943-02 photomultiplier, which has a monotonic response from 200–850 nm.

The C K-edge XANES of CNCs recorded in TEY is displayed in Fig. 2a, together with that of CNT, the starting material, the chemical vapor deposition (CVD) nanodiamond film reported earlier [2] and natural diamond (0.39 carat opaque yellow, from Sierra Leone). Let us first compare the XANES of CNC with that of CNT. The peaks centered at  $\sim 285$  and  $\sim 291$  to  $\sim 292$  eV can be assigned to  $1s$  electron transition to unoccupied  $\pi^*$  and  $\sigma^*$  orbitals, respectively, as is clearly displayed in the graphite-like CNT spectrum. The  $\pi^*$  transition in CNCs is unmistakably present although the  $\sigma^*$  is obscured by several other nearby transitions. The  $\pi^*$  transition is a direct evidence for the existence of graphitic  $\pi$  bonds in CNCs, which is in good agreement with previous HRTEM, diffraction and Raman observations [3]. The peak ratio of  $\pi^*$  to  $\sigma^*$  in CNCs is obviously lower than the ratio in randomly oriented CNTs. This observation can be attributed to the presence of amorphous carbon, and nitrogen [12] in CNCs, which donates electron charge to the  $\pi^*$

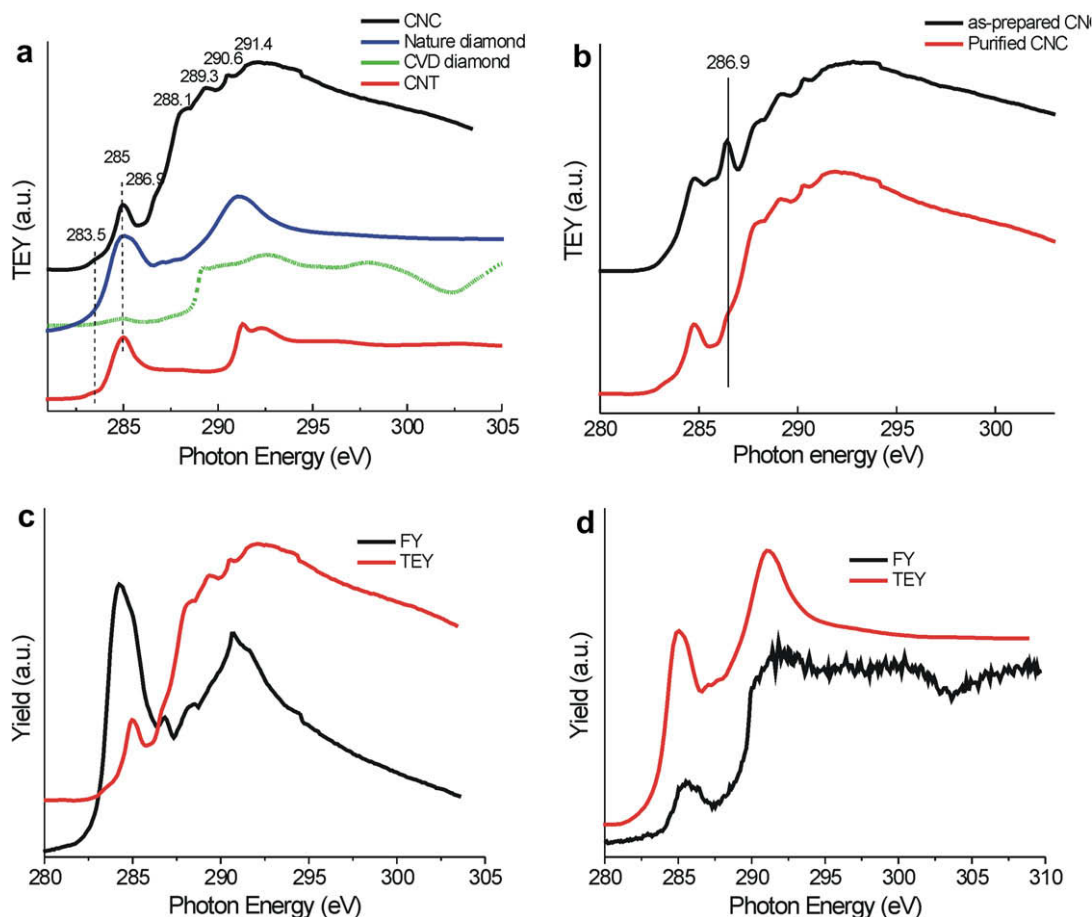


Fig. 2. (a) The C K-edge XANES of the purified carbon nanocrystals (CNC), CNTs, CVD nanodiamond and natural diamond obtained in TEY. (b) TEY of as-prepared CNC and purified CNC. (c) TEY and FY for CNC, and (d) TEY and FY for natural diamond.

states. Between the  $\pi^*$  and  $\sigma^*$  resonance, several rather sharp transitions are observed in the CNC spectrum. The band at  $\sim 286.9$  eV is most likely due to the  $1s$  to  $\pi^*$  transition of the carbon in the  $C\equiv N$  bond in acetonitrile or the  $C-H$  bond  $\sigma^*$  transition [16] from the electrolyte. Interestingly this transition intensity was reduced significantly upon CNC purification (Fig. 2b), which shows that nanocrystal purification using water extraction is effective. The peaks at  $\sim 288.1$  and  $\sim 289.3$  eV are assigned to the  $C=O$   $\pi^*$  transition [16,18,19] in CNCs resulting from oxidation, forming carboxylic groups on the surface. It should be noted that similar spectroscopic features have been observed in nitrogen doped CNTs and assigned to the carbon–nitrogen  $\pi^*$  transition [20]. The C K-edge  $\pi^*$  resonance for C–N interaction, for example, is at a photon energy very similar to that in graphite. Thus the N K-edge we present below will be a more site specific probe for nitrogen than the C K-edge. The existence of carbon–oxygen bonding feature in CNCs, especially in TEY is not uncommon since these groups are associated with surface defects and are also observed in CNTs [16]. In fact, high purity CNTs exhibit no features between the  $\pi^*$  and  $\sigma^*$  resonance. Our electrochemical treatment leading to the formation of CNCs will generate such groups via oxidation. A pre-edge transition, shown as a shoulder at  $\sim 283$  eV, appears in many carbon materials, and was previously attributed to the defect states of disordered carbon (amorphous) [21], for instance, dangling bonds or core-level excitons [22].

The CNC peak at  $\sim 290.6$  eV is not observable in CNTs. This transition is assigned to the pyridine-like unsaturated carbon–nitrogen HOMO + 1 orbital, providing spectroscopic evidence that  $sp^2$  C–N bonding exists in the CNCs. It also supports our notion described above on reducing the relative  $\pi^*$  intensity by an electron doping element. This point is supported by N K-edge XANES measurements discussed below.

We now examine the XANES of the natural diamond and CNC in the surface and bulk sensitive TEY and FY detection, respectively (Fig. 2c and d). It is immediately apparent from Fig. 2c that the FY XANES of the CNCs is graphitic-like although it still contains intense spectral features between the  $\pi^*$  and  $\sigma^*$  resonance, consistent with the presence of C–N and C–O interaction. Interestingly, Fig. 2d shows that graphitic carbon dominates the surface signal of natural diamond as inferred from the broad  $\pi^*$  and  $\sigma^*$  resonance in the TEY spectrum with no noticeable diamond features while the FY shows the unmistakable spectral feature of diamond, similar to that for CVD nanodiamond shown in Fig. 2a. Some noticeable  $sp^2$  carbon signal ( $\pi^*$  at  $\sim 285$  eV) is observed in the natural diamond, more intense than in CVD diamond (Fig. 2a). This observation indicates that the natural diamond sample contains  $sp^2$  C, which, despite a complex origin (vacancies, N doping etc.) is responsible for the luminescence.

Evidence for the presence of N in the CNC is confirmed by the N K-edge spectra recorded in both TEY and FY modes shown in Fig. 3. The XANES can be divided into two regions: the sharp resonance region at  $\sim 400$  eV and a broad peak at 407 eV. The former are transitions from  $1s$  to unoccupied  $\pi^*$  states and the latter corresponds to transition into the  $\sigma^*$  states and its energy position is sensitive to the bond length between N and C [12,18]. This is undoubtedly a direct evidence for the presence of nitrogen, forming unsaturated carbon–nitrogen bonds in the CNCs. The three  $\pi^*$  peaks at 399, 400 and 402 eV have been observed in various N containing carbon structures. They are attributable to pyridine-like, molecular nitrogen, and graphite-like bonding in the nitrogenated carbon materials, respectively, by comparison with model compounds [12,18,23]. Interestingly the graphitic feature at 402 eV is more bulk like as seen in the comparison between the surface sensitive TEY and the bulk sensitive FY XANES, the latter exhibits no thickness effect (broadening). Compared with the C K-edge XANES which contains contribution from amorphous carbon impurities,

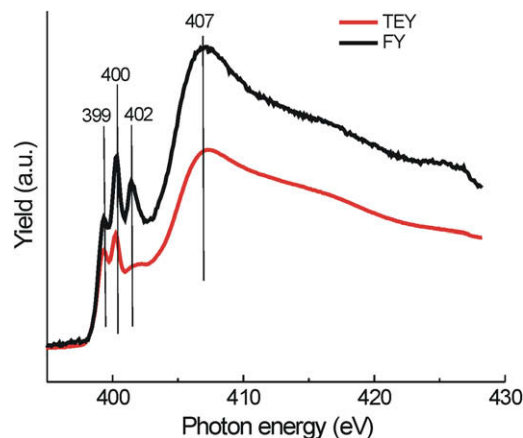
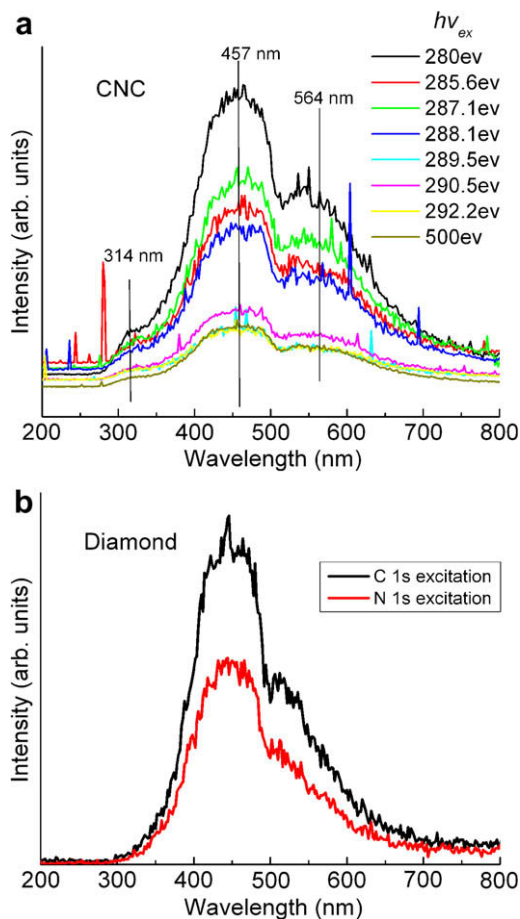


Fig. 3. The N K-edge XANES of the purified carbon nanocrystals (CNC) obtained in TEY and FY.

the similarity between TEY and FY XANES at the N K-edge clearly shows that N is incorporated uniformly in the CNCs. It should also be noted that the energy position of the  $\sigma^*$  resonance (407 eV), which is sometimes known as the shape resonance, and is associated with bond length (based on scattering theory, wherein the farther away the position of the resonance is above threshold, the shorter the bond), is at considerable lower energy than that of  $HC\equiv N$  ( $\sigma^*$ , 420.8 eV; IP, 406.8 eV) but further away from that of pyridine ( $\sigma^*$ , 408.4 eV; IP, 405.2 eV), indicating that N–C does not form triple bond, but forming C–N bonds with similar length to that in pyridine, in support of  $sp^2$  C–N bonding. There are two nitrogen containing entities (acetonitrile and tetrabutyl ammonium perchlorate) present in the electrochemically process for making CNCs<sup>3</sup>. The N K-edge data shown here favors the incorporation of N from ammonium ion rather than acetonitrile, which has a triple bond [3], although we can not eliminate C–N products resulting from reactions between acetonitrile and defects in CNT during the electrochemical cycling.

Finally the perhaps most interesting result is the similarity of XEOL from CNCs compared with that of natural diamond. Fig. 4a and b show, respectively, the XEOL from CNC and diamond excited with selected photon energies across the C and N K-edge. Since these data are normalized to the incoming photon flux, the drop in intensity across the C K-edge (from 280 eV to  $>285.5$  eV) in CNC indicates a reduction in the quantum efficiency for the luminescence per photon absorbed; this reduction in luminescence intensity with excitation photon energy across the edge is largely due to the truncation of the secondary process following X-ray excitation (Auger and fluorescence X-rays impart their energy to the optical channel). Since the thermalization of secondary electrons and holes significantly contribute to luminescence of a defect origin as is expected in the CNC and the probing depth reduces abruptly at the C K-edge resonance (the one absorption length reduces from  $\sim 2.4$   $\mu\text{m}$  to  $\sim 90$  nm across the edge) [26], the thermalization track will terminate more abruptly above the absorption edge as a larger fraction of Auger electrons and fluorescence X-rays will escape the solid making no contribution to the luminescence. It should be noted that despite the variation in overall intensity, the branching ratio (intensity of an individual peak divided by the total intensity across the spectrum) of all the peaks is exactly the same, independent of the excitation energy. In other words, when all spectra are normalized to the maximum peak height, they are identical. There are three emission bands around 314 nm, 457 nm and 564 nm, respectively. The details are discussed below. The diamond sample exhibits similar luminescence at first glance and, as is the case for CNC, there is also no excitation energy



**Fig. 4.** (a) XEOL from CNC excited by a range of photon energies from 280 eV below the C K-edge to 500 eV above the N K-edge and (b) XEOL from natural diamond excited at the C and N K-edge.

dependence in the branching ratio of the luminescence peaks. Before we proceed with the comparison, we must note that luminescence from diamond is well studied and it is not our intention here to discuss it in detail. We merely want to focus on the peculiar similarity in XEOL between CNC and natural diamond.

Fig. 4b shows the XEOL from diamond excited with photon energy at the C and N K-edges. Diamond has a wide band gap (indirect, 5.5 eV~225 nm). No near band gap emission is observed as expected. However, luminescence from impurity/defect states within the band gap is common. Close observation of Fig. 4b reveals a blue emission band at 450 nm (2.75 eV) and shoulders in the yellow at 520 nm (2.38 eV) and 570 nm (2.17 eV), comparable to luminescence from the well known N3 center (3 N atoms bonded to a C vacancy) and C center of diamond (a nitrogen atom occupying a substitution site, a deep donor state at ~2.2 eV below the bottom of the conduction band), respectively [27].

We now compare the XEOL of CNC with that of natural diamond and previously reported CVD diamond in Fig. 5a. It is interesting to note that the XEOL of CNC is in close resemblance to that of natural diamond and fairly close to that of CVD nanodiamond as well. The XEOL of CNC resembles previously reported photoluminescence (425 nm, 2.92 eV) in solution with a dominant but broadened and slightly shifted emission at ~455 nm (2.7 eV)<sup>3</sup> with the exception that two additional features are presented: (1) the weak emission shown as a shoulder at 314 nm (3.9 eV) and (2) a yellow emission band at 564 nm (2.2 eV). The weak emission at 314 nm has also been observed in the CVD nanodiamond [2] and is a well established silicon-impurity-related emission. The yellow emission

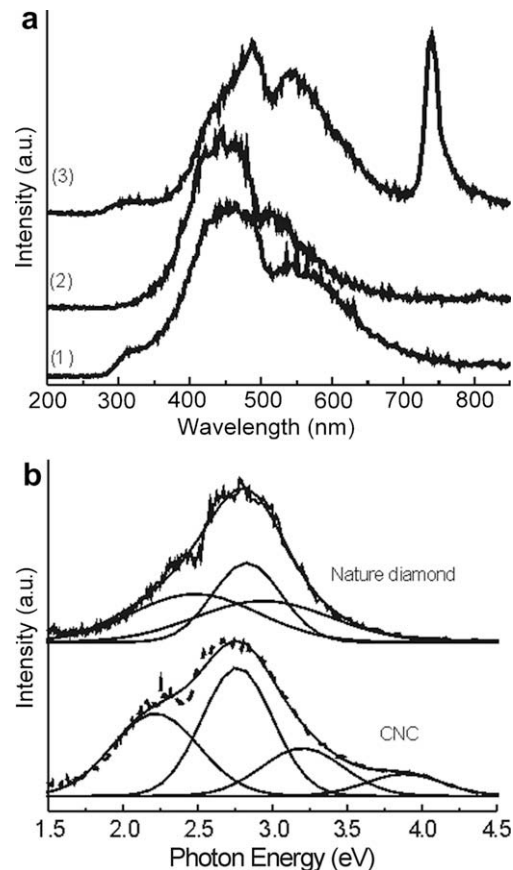


**Fig. 5.** (a) Room temperature XEOL from the purified carbon nanocrystals (CNC) (1), and natural diamond (2) excited at 280 eV and CVD nanodiamond film grown on Si wafer excited at 500 eV (3) (from Ref. [2]). (b) Detailed XEOL comparison of CNC and natural diamond.

is red-shifted relative to natural diamond but in line with CVD nanodiamond. This emission is probably quenched by solvent in solution or more accessible with X-ray excitation in the solid state. The sharp emission at 743 nm (1.67 eV) for the CVD diamond is a well established silicon-impurity-related emission due to diffusion of silicon into diamond during the deposition [2]. Thus, the XEOL of CNCs reproduces all similar transition bands in natural diamond and CVD diamond, both of which are known to contain N impurities.

Fig. 5b provides Gaussian fits of the XEOL of CNC (4 peaks) and natural diamond (3 peaks) in eV. We see that the blue emission from CNC at ~2.75 eV can be easily identified with that of the diamond XEOL. The yellow emission at ~2.2 eV is red-shifted relative to natural diamond. The UV emission at 3.95 eV seen in CNC is absent in diamond. There is another UV band at 3.25 eV which is more intense in CNC than in diamond where it broadens considerably due to overlap of many possible defect states in bulk natural diamond. This peak could be analogous to emission of the A center, a common defect in natural diamonds consisting of a pair of nitrogen atoms substituting for the carbon atoms. The A center lies ~4 eV below the conduction band [27]. Based on the similarities (nearly same Gaussian peaks position and intensity ratios) in XEOL between CNC and diamond, we propose that the N-bonded carbon acts as luminescence center in CNCs, analogous to the N defects in CVD nanodiamond and natural diamond. Generally, CVD diamond [24] and natural diamond [25] are known to contain nitrogen and nitrogen related defects. Our results provide direct evidence that the CNCs prepared according our procedure contain nitrogen, which acts as a luminescence center. Thus, our results show that

luminescence from all the above samples can have a similar origin, the N-bonded carbon, although the dominated phase in the CNC sample is  $sp^2$  bonded carbon. What remains puzzling is that natural diamond and CVD diamond thin film have a dominant cubic structure with primarily  $sp^3$  bonding. Further insight awaits experiments to explore the local structure and the effect of N impurities in  $sp^3$  and  $sp^2$  chemical environments of carbon.

In conclusion, we have applied XANES and XEOL to elucidate the electronic structure of blue luminescent CNCs. XANES results show that CNC is essentially graphitic but contains an oxidized surface and N impurities throughout the nanostructure. XANES also show that the yellow natural diamond has a graphitic surface while its bulk has a cubic diamond structure with some  $sp^2$  content resulting from defects/impurities. XEOL results suggest that N (most likely from tetrabutyl ammonium ion) incorporated into the CNC ( $sp^2$  bonded carbon dominates) is responsible for the luminescence. XEOL has also confirmed that N impurity is the origin of luminescence from natural diamond and CVD diamond, which almost certainly involves N-associated defects.

### Acknowledgements

Works done in UWO are financially supported from NESRC, CFI, OIT, OPT, PREA, and CRC (T.K.S.). CLS is supported by NSERC, NRC, CHIR, and the University of Saskatchewan.

### References

- [1] R.H. Baughman, A.A. Zakhidov, W.A. de Heer, *Science* 297 (2002) 787.
- [2] X. Zhou et al., *J. Am. Chem. Soc.* 129 (2007) 1476.
- [3] J. Zhou, C. Booker, R. Li, X. Zhou, T.-K. Sham, X. Sun, Z. Ding, *J. Am. Chem. Soc.* 129 (2007) 744.
- [4] Y.-P. Sun et al., *J. Am. Chem. Soc.* 128 (2006) 7756.
- [5] Y. Lin et al., *J. Phys. Chem. B* 109 (2005) 4779.
- [6] J.X. Cheng, Y. Fang, Q.J. Huang, Y.J. Yan, X.Y. Li, *Chem. Phys. Lett.* 330 (2000) 262.
- [7] Y. Sun, S.R. Wilson, D.I. Schuster, *J. Am. Chem. Soc.* 123 (2001) 5348.
- [8] F. Zhang, Y. Fang, *J. Phys. Chem. B* 110 (2006) 9022.
- [9] G. Schick et al., *J. Am. Chem. Soc.* 121 (1999) 246.
- [10] J.E. Riggs, Z. Guo, D.L. Carroll, Y.-P. Sun, *J. Am. Chem. Soc.* 122 (2000) 5879.
- [11] S.J. Henly, *Appl. Phys. Lett.* 85 (2004) 6236.
- [12] R. McCann, *Diamond Relat. Mater.* 14 (2005) 1057.
- [13] Z. Li, L. Zhang, D.E. Resasco, B.S. Mun, F.G. Requejo, *Appl. Phys. Lett.* 90 (2007) 103115/103111.
- [14] M. Imamura et al., *Phys. B: Condens. Matter (Amsterdam)* 208&209 (1995) 541.
- [15] J.W. Chiou et al., *Appl. Phys. Lett.* 81 (2002) 4189.
- [16] J. Zhou et al., *Chem. Phys. Lett.* 437 (2007) 229.
- [17] T.K. Sham et al., *Nature* 363 (1993) 331.
- [18] S.S. Roy, P. Papakonstantinou, T.I.T. Okpalugo, M.J. Murphy, *Appl. Phys.* 100 (2006) 053703.
- [19] B. Bouchet-Fabre et al., *Diamond Relat. Mater.* 14 (2005) 881.
- [20] T.M. Minea, B. Bouchet-Fabre, S. Lazar, S. Point, H.W. Zandbergen, *J. Phys. Chem. B* 110 (2006) 15659.
- [21] S.C. Ray, J.W. Chiou, W.F. Pong, M.H. Tsai, *Crit. Rev. Solid State Mater. Sci.* 31 (2006) 91.
- [22] R. Gago et al., *Phys. Rev. B* 72 (2005) 14120.
- [23] J. Stohr, *NEXAFS Spectroscopy*, Springer, Berlin, 1992, p. 106.
- [24] D.G. Kim, T.Y. Seong, Y.J. Baik, M.A. Stevens Kalceff, M.R. Phillips, *Diamond Relat. Mater.* 8 (1999) 712.
- [25] W. Kaiser, W.L. Bond, *Phys. Rev.* 115 (1959) 857.
- [26] T.K. Sham, S.J. Naftel, I. Coulthard, in: T.K. Sham (Ed.), *Chemical Applications of Synchrotron Radiation Part II*, World Scientific Singapore, 2002, p. 1154.
- [27] J. Walker, *Rep. Progr. Phys.* 42 (1979) 1605.